Structures, Structural Dynamics, and Materials and Co-located Conferences
April 8-11, 2013, Boston, Massachusetts
54th AIAA/ASME/ASCE/AHS/ASC Structures, Structural Dynamics, and Materials Conference

Development of modeling for Cable Harnessed Structures

Jiduck Choi[1]
Virginia Tech, Blacksburg, Virginia, 24061, USA

and

Daniel J. Inman[2]
University of Michigan, Ann Arbor, Michigan, 48109, USA

In Satellite applications, modeling is extremely important in order to predict behavior during launch and in orbit. Today detailed finite element models of satellites are accurate and agree well with experimental data. However once the satellites are hung with cable harnesses, the ability to model the system dynamics has eluded modeling engineers. Here we investigate in a simple way the effects of adding cables to a simple structure with the goal of developing an understanding of the physics of cables interacting with a structure. In this paper, we present Spectral Element Method (SEM) approach to accomplish the modeling of cable harnessed structure. The cable harnessed structure is considered as a double beam system with both beams connected by spring at specific locations to emulate the effect of attaching cables to the satellite structure. First, the SEM is applied and compared with the conventional FEM. Based on the exact solutions of the governing equation of the element, SEM has much better accuracy in higher frequencies. SEM shows the extremely high accuracy with minimum number of DOFs. Next, the validation of SEM approach was conducted by using comparison with experimental measurement. Last, the changes of damping matrices were investigated to obtain the effect on the damping due to attaching the cable bundles.

I. Introduction

To obtain the predictive and accurate modeling of a cable harnessed structure. A cable harnessed structure is simplified and considered as a double beam system to emulate the effect of attaching cables to the structure. The response of single beam has an exact solution, which can be obtained in various ways [1]. However, when a secondary beam is attached to the main beam by means of several spring connections, obtaining the solution of system becomes more complicated. Several authors have investigated double-beam systems elastically combined by a distributed spring in parallel. Seelig and Hoppman II [2], worked out the solution of differential equation of elastically connect parallel beams. Gürgöze [3], [4] dealt with the derivation of the frequency equation of a clamped-free Euler Bernoulli beam with several spring-mass systems attached in mid of span by means of the Lagrange multipliers method. Vu [5] presented an exact method for the vibration of a double-beam system subject to harmonic excitation. The system consists of a main beam with an applied force, and an auxiliary beam, with a distributed spring k and damper c in parallel between the two beams. Wu and Whittaker [6] considered the beam connected with two degrees-of-freedom systems at specific locations.

An important problem is to determine the best way to model the connection between the two beams (called cable ties in the literature) To find the cable properties and proper modeling, Coombs [7] conducted the experiments and showed that the Timoshenko beam theory was most appropriate for modeling cables.

Rao [8] considered the free response of several Timoshenko beam systems. Doyle [9] and Lee [10] present excellent texts on the spectral element method. Doyle introduced the basic formulation of spectral element matrix by using an Euler-Bernoulli beam. Lee summarized the various ways to derive the spectral element matrix for structural elements such as Euler beam, Timoshenko beam and plate. Lee also presented several practical applications of SEM. Many authors have used the dynamic stiffness approach to modeling, which is very closely related to the SEM

[1] Ph.D. candidate, Department of Mechanical Engineering, jdchoi@vt.edu, AIAA Student member
[2] Professor, Chair, Department of Aerospace Engineering, DanInman@umich.edu, AIAA Fellow

approach. Banerjee [11] and Chen [12] used the dynamic stiffness matrix for the beam with attached two DOF systems. Li and Hua [13], [14] considered elastically connected two and three parallel beams by using dynamic stiffness analysis. Jiao et al [15] investigated the Euler beam with an arbitrary cross section.

This paper is organized as follows. In Section II, the simplified model of a cable harnessed structure is introduced. In Section III, the Spectral Element Method for a single beam is introduced. And its validation is performed with numerical model and experiment. Once validated, the SEM approach has extended to double beam system. In section IV, The cable attachment is considered as a beam to simplify the material properties of cable bundles. The numerical analysis is conducted and the experiment with the real double beam system is presented. The FRF measurement data is compared with those of SEM. Through section III, IV, Through the SEM approach, we can obtain an accurate result with a minimum number of DOFs. In addition, this approach may be considered as a numerically "exact" solution because the SEM is based on the exact solutions of the governing differential equation of the element.

Lee [16], [17] presented the experimental method to identify the damping matrices. In section V, the change of damping matrices was investigated, which reveals the effect on the damping due to adding a cable bundles. Closing remarks and future perspectives are briefly outlined in Section VI.

II. Description of the Model

A simplified model of a cable harnessed structure is shown in Figure 1. The main structure is modeled as a beam with rectangular cross section. The cable attachment is treated as a circular beam. The interconnections between beams can be defined by means of their location and their spring constants. By utilizing this model, the SEM for a combined system will be validated and compared with the FEM results.

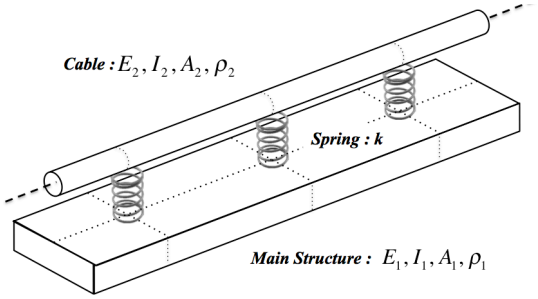

Figure 1. The model of a cable harnessed structure

III. Spectral Element Method for Timoshenko Beam

A. Formulation

The equation of motion of the Timoshenko beam can be expresses as

$$\begin{aligned} \kappa GA\left(w'' - \theta'\right) - \rho A\ddot{w} &= 0 \\ EI\theta'' + \kappa GA\left(w' - \theta\right) - \rho I\ddot{\theta} &= 0 \end{aligned} \tag{1}$$

where w and θ are the transverse deflection and the slope respectively. The solutions of equation (1) in spectral form are:

$$w(x,t) = \frac{1}{N}\sum_{n=0}^{N-1} W_n(x) e^{i\omega_n t}, \quad \theta(x,t) = \frac{1}{N}\sum_{n=0}^{N-1} \Theta_n(x) e^{i\omega_n t} \tag{2}$$

And the spatial solution $W(x)$ and $\Theta(x)$ can be written as

$$W(x) = a_1 e^{-j\beta_1 x} + a_2 e^{-j\beta_2 x} + a_3 e^{-j\beta_3 x} + a_4 e^{-j\beta_4 x}$$
$$\Theta(x) = a_1 b_1 e^{-j\beta_1 x} + a_2 b_2 e^{-j\beta_2 x} + a_3 b_3 e^{-j\beta_3 x} + a_4 b_4 e^{-j\beta_4 x} \tag{3}$$

Substituting equation (2), (3) into (1) yields the relation between b and β to be

$$\begin{bmatrix} \kappa GA\beta_i^2 - \rho A\omega^2 & -j\kappa GA\beta_i \\ j\kappa GA\beta_i & EI\beta_i^2 + \kappa GA - \rho I\omega^2 \end{bmatrix} \begin{Bmatrix} 1 \\ b_i \end{Bmatrix} = \begin{Bmatrix} 0 \\ 0 \end{Bmatrix} \quad (i = 1,2,3,4) \tag{4}$$

The nodal displacement and slope at both ends can be expressed by

$$\{d\} = \begin{Bmatrix} W(0) \\ \Theta(0) \\ W(L) \\ \Theta(L) \end{Bmatrix} = \begin{bmatrix} 1 & 1 & 1 & 1 \\ b_1 & b_2 & b_3 & b_4 \\ e^{-j\beta_1 L} & e^{-j\beta_2 L} & e^{-j\beta_3 L} & e^{-j\beta_4 L} \\ b_1 e^{-j\beta_1 L} & b_2 e^{-j\beta_2 L} & b_3 e^{-j\beta_3 L} & b_4 e^{-j\beta_4 L} \end{bmatrix} \{a\} = [D(\omega)]\{a\} \tag{5}$$

where $\{a\} = \begin{bmatrix} A & B & C & D \end{bmatrix}^T$. The shear force and moments are $V(x,t) = \kappa GA\left(W'(x) - \Theta(x)\right)$ and $M(x,t) = EI(x)\Theta'(x)$. Thus the transverse shear force and bending moments at the nodal points are given by

$$\{f\} = \begin{Bmatrix} -V(0) \\ -M(0) \\ V(L) \\ M(L) \end{Bmatrix} = \begin{bmatrix} -\kappa GA(b_1 - j\beta_1) & -\kappa GA(b_2 - j\beta_2) & -\kappa GA(b_3 - j\beta_3) & -\kappa GA(b_4 - j\beta_4) \\ jEI\beta_1 b_1 & jEI\beta_2 b_2 & jEI\beta_3 b_3 & jEI\beta_4 b_4 \\ \kappa GA(b_1 - j\beta_1)e^{-j\beta_1 L} & \kappa GA(b_2 - j\beta_2)e^{-j\beta_2 L} & \kappa GA(b_3 - j\beta_3)e^{-j\beta_3 L} & \kappa GA(b_4 - j\beta_4)e^{-j\beta_4 L} \\ jEI\beta_1 b_1 e^{-j\beta_1 L} & jEI\beta_2 b_2 e^{-j\beta_2 L} & jEI\beta_3 b_3 e^{-j\beta_3 L} & jEI\beta_4 b_4 e^{-j\beta_4 L} \end{bmatrix} \{a\} = [F(\omega)]\{a\} \tag{6}$$

By means of equation (6), the spectral element matrix of the Timoshenko beam can be obtained. By following the same procedure, the spectral element matrix for Euler-Bernoulli beam can also be obtained.

B. Numerical Analysis

The conventional FEM and spectral beam elements will be compared using a simple example to validate the efficiency of the SEM. Previous research has focused on the clamped-free or simply supported case. Here we are concerned with the free vibration of free-free beam, which is analyzed using both types of elements. The material used in the example is aluminum with elastic modulus of $7 \times 10^{10}\ N/m^2$ and density of $2700\ kg/m^3$. The dimensions of beam are $1.2192 \times 0.0254 \times 0.003175\ (m)$. From the characteristic equation of free-free beam [1], $\cos(\beta L)\cosh(\beta L) = 1$, the exact natural frequencies are calculated. And the root-finding algorithms [18] are used to find the ω_n in SEM.

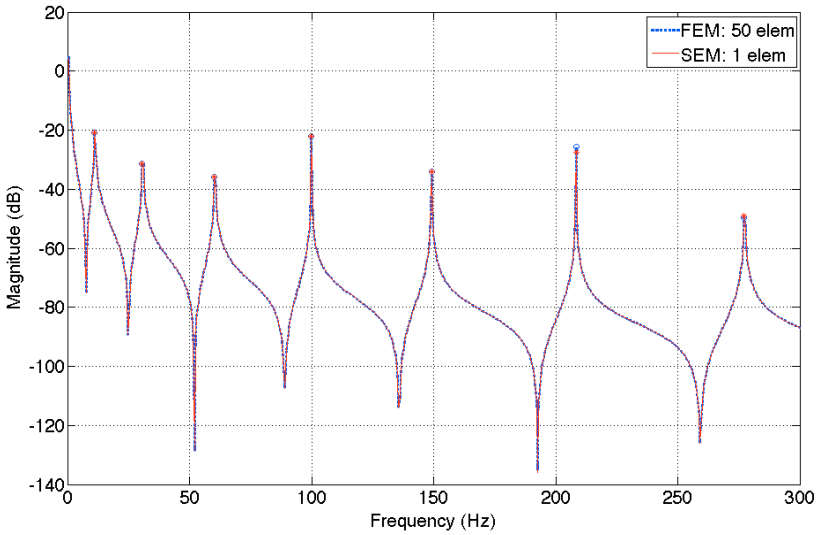

Figure 2. Comparison of FEM (blue dot) and SEM (red)

Table 1. Natural frequencies (Hz) of exact solution, SEM and FEM

Mode	ω_{exact}	$\omega_{spec.}$	ω_{FEM} (10)	ω_{FEM} (30)	ω_{FEM} (50)
1	0	0	0.00001	0.00009	0.0002
2	11.1794	11.1794	11.1798	11.1794	11.1794
3	30.8165	30.8165	30.8242	30.8166	30.8165
4	60.4127	60.4127	60.4683	60.4135	60.4128
5	99.8654	99.8654	100.1052	99.8687	99.8658
6	149.5272	149.1817	149.9387	149.1928	149.1831
7	208.3612	208.3612	210.2857	208.3915	208.3652
8	277.4040	277.4040	281.5237	277.4749	277.4134

The natural frequencies of free-free beam are compared in Table 1. The SEM results are identical to the exact solution. As the number of elements is increased the FEM results go closer to the SEM results and the exact solution. In **Figure 2**, FEM use 50 Element and SEM use only one element. Both results show good agreement. Considering the high frequency range, the more elements are necessary to obtain the good results in the FEM. This means that SEM can predict the dynamics of a system with minimum number of D.O.Fs.

C. Experimental Validation

To validate the accuracy of SEM, The Frequency Response Function (FRF) was measured with experimental setup as shown in **Figure 3**. The experiment was conducted by using PCB impact hammer, Polytec Laser vibrometer and its controller, and RT pro measurement software. The test specimen is 34-inch long Al beam with the cross section of 1-inch width and 1/8 inch thickness. The material properties of specimen are shown in **Table 2**. The FRFs were measured at total 9 points.

Table 2. Material properties of Al single beam

	L (m)	A (m^2)	I (m^4)	E (GPa)	G (GPa)	ρ (kg/m^3)	κ
Al Beam	0.8636	8.0645e-05	6.7746e-11	70	46	2700	0.889

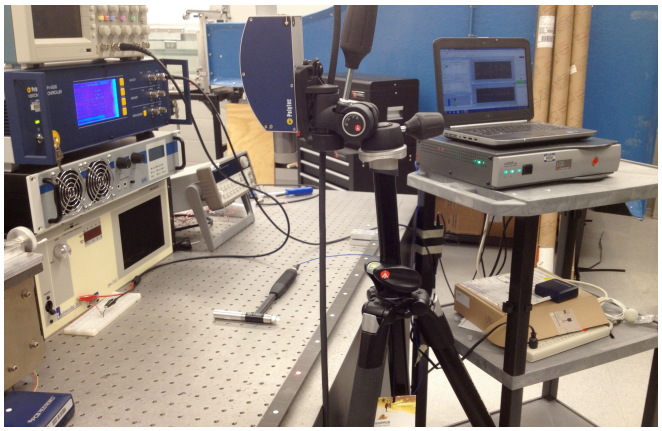

Figure 3. Experimental configuration

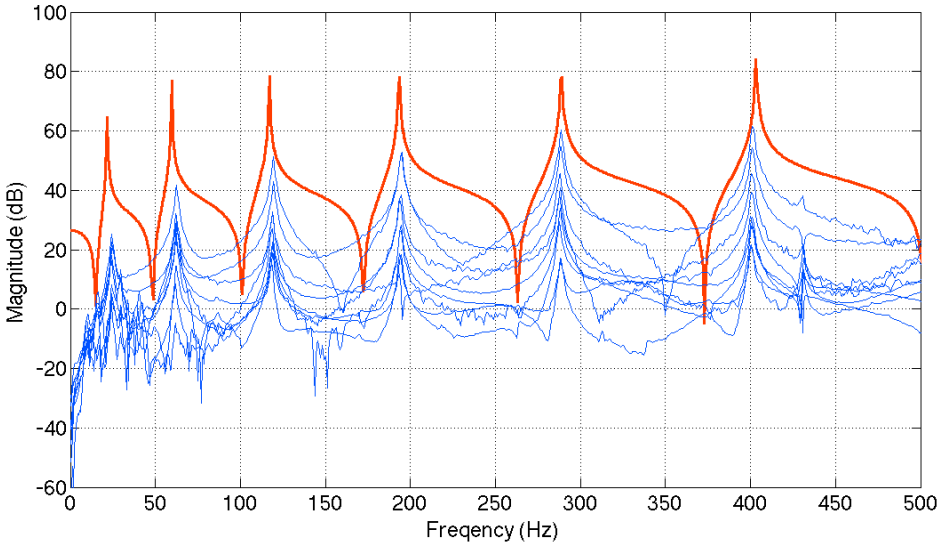

Figure 4. FRF from measurement (blue) and SEM (red bold)

Figure 4 shows the FRF from the measurement data and Spectral Element method. The peaks present the natural frequency of the experiments and analytical model. Both results show good agreements. We can conclude that the SEM can present the accuracy results.

IV. Spectral Element Method for a Combined System

A. Formulation

In many papers ([2], [5], [8], [13], [14]), a double beam was considered such that two beams are connected with numerous distributed springs. However, Author [19] has presented the SEM approach to define the specific locations at that the connections exist. The effect of number of connections and the stiffness of connection has also been investigated by numerical analysis. Through the definition of locations of interconnections, the simplified model can reflect the real structure more realistically. **Figure 5** illustrates the specific connection points. A specific set of locations are defined in or that the effect of the number and locations of connection can be identified and studied.

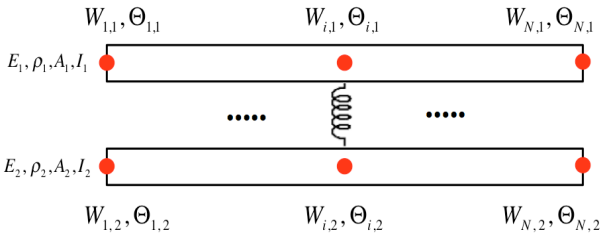

Figure 5. Double Beam Model

After obtaining the spectral element matrix from equation (6), we can assemble elements to generate the global spectral matrix. And we apply the boundary conditions to the global system. The global system can be expressed by

$$\left[S_g\right]\left\{d_g\right\} = \left\{f_g\right\} \tag{7}$$

Considering the double beam system in **Figure 5**, each beam is *2N* D.O.F. system where *N* is total number of nodes. And the spring connection exists between i^{th} nodes of beam 1 and 2. For beam 1 and 2, we can formulate the global stiffness matrix by means of equation (7). From the relation between nodal displacement and force, the combined global stiffness matrix without the spring connections is

$$\begin{bmatrix} S_{g,1} & 0 \\ 0 & S_{g,2} \end{bmatrix} \begin{Bmatrix} \{d_{g,1}\} \\ \{d_{g,2}\} \end{Bmatrix} = \begin{Bmatrix} \{f_{g,1}\} \\ \{f_{g,2}\} \end{Bmatrix} \tag{8}$$

where

$$\begin{aligned} \{d_{g,1}\} &= \begin{bmatrix} W_{1,1} & \Theta_{1,1} & \cdots & W_{i,1} & \Theta_{i,1} & \cdots & W_{N,1} & \Theta_{N,1} \end{bmatrix}^T \\ \{d_{g,2}\} &= \begin{bmatrix} W_{1,2} & \Theta_{1,2} & \cdots & W_{i,2} & \Theta_{i,2} & \cdots & W_{N,2} & \Theta_{N,2} \end{bmatrix}^T \\ \{f_{g,1}\} &= \begin{bmatrix} V_{1,1} & M_{1,1} & \cdots & V_{i,1} & M_{i,1} & \cdots & V_{N,1} & M_{N,1} \end{bmatrix}^T \\ \{f_{g,2}\} &= \begin{bmatrix} V_{1,2} & M_{1,2} & \cdots & V_{i,2} & M_{i,2} & \cdots & V_{N,2} & M_{N,2} \end{bmatrix}^T \end{aligned} \tag{9}$$

The global stiffness matrix of each beam, $S_{g,1}$ and $S_{g,2}$, are *2N×2N* matrices and the global displacement and force vector $d_{g,1}, d_{g,2}, f_{g,1}$ and $f_{g,2}$ are *2N×1* vectors. The force f_i between the i^{th} nodes of beam 1 and beam 2 due to the spring connection, f_i is

$$f_i = k(W_{i,1} - W_{i,2}) \tag{10}$$

Considering the relation of force and displacement, the total combined system can be expressed as

$$\begin{aligned} \left[S_{g,1}\right]\left\{d_{g,1}\right\} + \sum_{i=1}^{p} f_i &= \left\{f_{g,1}\right\} \\ \left[S_{g,2}\right]\left\{d_{g,2}\right\} - \sum_{i=1}^{p} f_i &= \left\{f_{g,2}\right\} \end{aligned} \tag{11}$$

where p is the total number of connections. Let $\{L_i\}$ denote a locator vector defining the location of the i^{th} connector. The vector $\{L_i\}$ is $4N\times 1$ vector correspondent with $[d_{g,1}\ d_{g,2}]^T$. The $2i\text{-}1^{th}$ component of $\{L_i\}$ is 1 and the $2N+2i\text{-}1^{th}$ component of $\{L_i\}$ is -1 and the remainders are zero.

$$\begin{bmatrix} S_{g,1} & 0 \\ 0 & S_{g,2} \end{bmatrix} \begin{Bmatrix} d_{g,1} \\ d_{g,2} \end{Bmatrix} + \sum_{i=1}^{p} k\{L_i\}\{L_i\}^T \begin{Bmatrix} d_{g,1} \\ d_{g,2} \end{Bmatrix} = \begin{Bmatrix} f_{g,1} \\ f_{g,2} \end{Bmatrix} \tag{12}$$

Owing to usage of the exact dynamic stiffness matrix to formulate the spectral element matrix, we can solve exactly for the system characteristics with a minimum number of element matrices. Now, we can calculate the natural frequencies by solving the eigenvalue problem for spectral element model given by

$$[S_g]\{d_g\} = 0 \tag{13}$$

Similar to the regular eigenvalue problem, setting the determinant of the global spectral matrix $[S_g]$ to zero, $\det(S_g(\omega_n)) = 0$, yields the natural frequencies ω_n. However, the spectral element matrix consists of transcendental functions such as sine, cosine, hyperbolic cosine (cosh), and hyperbolic sine (sinh). Thus the linear eigensolver such as 'eig' in MATLAB cannot be used. The several approaches to find the eigenvalues are summarized by Lee [10].

B. Numerical analysis

A free vibration of free-free double beam will be analyzed for a combined system with 5 connections. For 5 connections case, the FEM used 60 elements and the SEM used 6 elements. The material properties of both beams are summarized in **Table 3**. The spring constant k is 10 N/m. Root-finding algorithms [18] are utilized to find the ω_n in the SEM. The natural frequencies for the following four cases are obtained.

- FEM: Euler-Euler beam and Euler-Timoshenko beam
- SEM: Euler-Euler beam and Euler-Timoshenko beam

Table 3. Material properties of Al beam and Copper rod

	L (m)	A (m^2)	I (m^4)	E (GPa)	G (GPa)	ρ (kg/m^3)	κ
Al Beam	1.2192	8.0645e-05	6.7746e-11	70	-	2700	-
Cu Beam	1.2192	7.9173e-06	4.9856e-12	117	46	8940	0.889

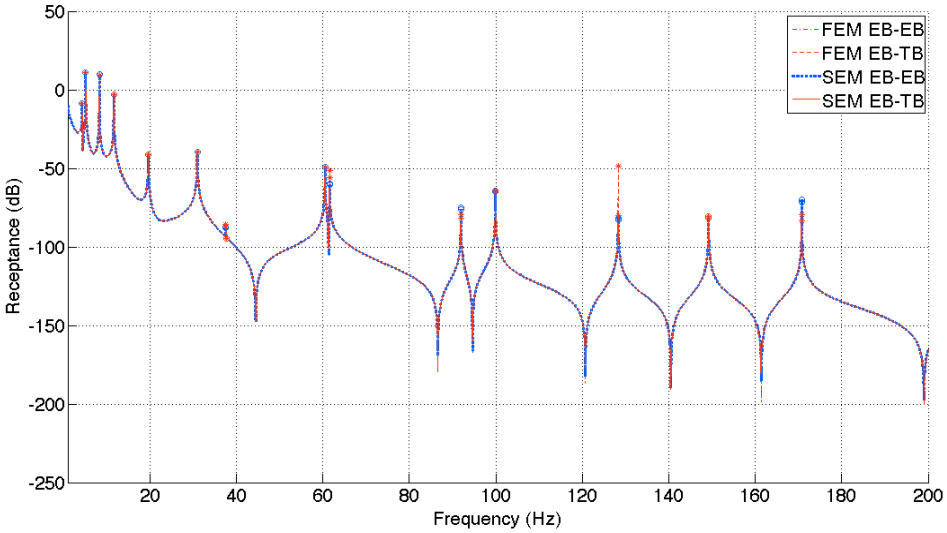

Figure 6. Comparison of 4 cases of Al beam + Cu beam (EB: Euler beam, TB: Timoshenko Beam)

Table 4. Natural frequencies of 4 cases for a combined system (Al beam+ Copper beam)

Mode	EB, TB	Euler	Timosh.	Euler-Euler		Euler-Timoshenko	
	Al	Cu	Cu	FEM	SEM	FEM	SEM
1	11.179	6.8806	6.8806	3.2156	3.2156	3.2156	3.2156
2	30.817	18.967	18.966	4.4891	4.4891	4.4891	4.4891
3	60.416	37.184	37.182	8.2777	8.2777	8.2777	8.2777
4	99.878	61.472	61.466	11.652	11.652	11.652	11.652
5	149.22	91.842	91.828	19.421	19.421	19.421	19.421
6	208.47	128.31	128.28	30.914	30.914	30.914	30.914
7	277.67	170.9	170.85	37.441	37.441	37.441	37.441
8	356.87	219.64	219.57	60.459	60.459	60.459	60.459
10	446.18	274.61	274.49	61.573	61.573	61.573	61.542
11	545.7	335.86	335.69	91.914	91.914	91.914	91.883
12	655.62	403.52	403.28	99.906	99.874	99.906	99.874
13	776.17	477.71	477.39	128.34	128.27	128.3	128.24
14	907.62	558.61	558.19	149.25	149.19	149.25	149.19

The results in **Table 4** show that the SEM gives very accurate results with a minimum number of elements compared with the FEM. In general SEM calculations require fewer elements than FEM to obtain higher frequencies.

C. Experimental validation

To validate the SEM results, the modal tests were conducted to obtain the FRF from two double systems.

1) Experiment 1: Two identical beams connected by 5 springs

The experimental configuration is shown in **Figure 7**. The free-free boundary condition applied to this experiment. Two identical Aluminum beams were used and connected by 5 springs that have a spring stiffness k=10 N/m. The springs are attached by using the Epoxy adhesive. The material properties are summarized in **Table 5**.

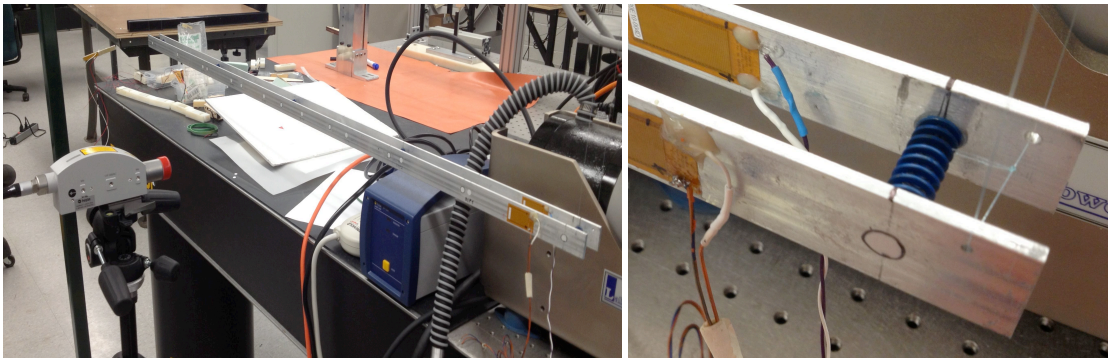

Figure 7. Experimental configuration

Table 5. Material properties of Aluminum beams

	L (m)	A (m^2)	I (m^4)	E (GPa)	G (GPa)	ρ (kg/m^3)	κ
Al Beam	1.2192	8.0645e-05	6.7746e-11	70	46	2700	0.889

To verify that both beams work as a combined system, MFC was actuated at the second beam and the FRF was measured at the first beam. **Figure 8** shows the FRF measurement. From the FRF, it was found that the two beams works together as a double beam system. The FRF from measurement and SEM present very close natural frequencies. We can conclude that the presented SEM approach can predict the dynamic behavior accurately.

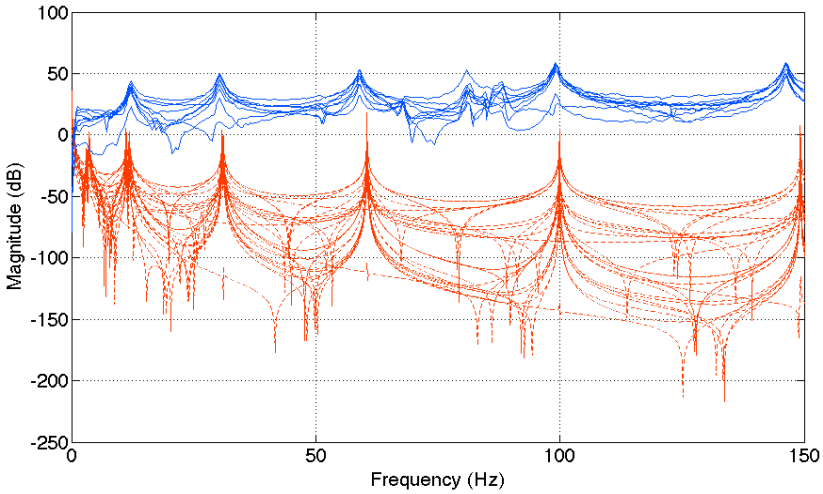

Figure 8. FRF from measurement (blue) and SEM (red dot)

2) Experiment 2: Al beam with Copper beam connected by tie-down and zip-tie

The experimental setup is the same with **Figure 3**. The clamped-clamped boundary condition applied to this experiment. In this experiment, the real connection was applied as shown in **Figure 9**. The FRFs were measured with 9 points. The 9x9 full FRF matrix was obtained. **Figure 10** shows the FRFs of measurement and SEM at point 1. The spring stiffness of connections was applied with the value of k=1 N/m. Both results show good agreement in natural frequencies. This shows the same results in previous test that the SEM presents the accurate prediction for the dynamic characteristics of a combined system.

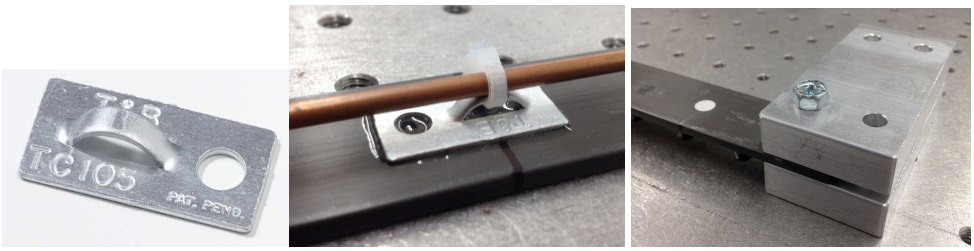

Figure 9. Tie-down connection and clamped B.Cs

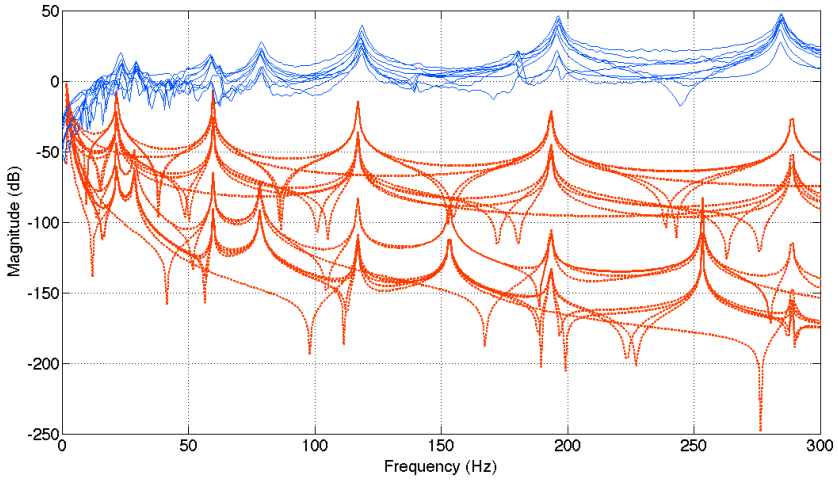

Figure 10. FRF of a double beam from measurement (blue) and SEM (red dot)

V. Identification of effect on damping matrices due to attaching cable bundle

A. Calculation of damping matrices from FRF measurement

Lee [16], [17] presented the way to calculate the damping matrices from measured FRF. The procedure to obtain the damping matrices can be summarized as followings. The equation of motion of a dynamic system with damping is:

$$M\ddot{x}(t)+C\dot{x}(t)+(K+jD)x(t)=f(t) \tag{14}$$

where M, K, C and D are the mass, stiffness, viscous damping and structural damping matrices. *x(t)* and *f(t)* are the displacement vector and the applied forces vector. For a harmonic excitation, *x(t)* and *f(t)* are shown:

$$x(t)=X(\omega)e^{j\omega t},\ f(t)=F(\omega)e^{j\omega t} \tag{15}$$

Substituting equation (16) into (15) yields

$$\left[\left(K-\omega^2 M\right)+j(\omega C+D)\right]X(\omega)=F(\omega) \tag{16}$$

The dynamic stiffness matrix (DSM) is expressed as

$$\left[H(\omega)^c\right]^{-1}=\left(K-\omega^2 M\right)+j(\omega C+D) \tag{17}$$

where $H(\omega)^c$ is the frequency response matrix (FRM) in the form of

$$H(\omega)^c=\left[H_{ij}^c\right]=\left[X_i/F_i\right],i,j=1,2,3,... \tag{18}$$

H_{ij}^c is the complex frequency response function (FRF) measured between the nodes *i* and *j*. The DSM is expressed as a inverse of measured complex FRM. FRM is much easier to measure than DSM. After the obtaing the DSM by inverting the FRM, Equation (17) can be express as

$$\text{imag}\left[H(\omega)^c\right]^{-1}=\omega C+D,\qquad \text{real}\left[H(\omega)^c\right]^{-1}=K-\omega^2 M \tag{19}$$

where imag and real represent the imaginary and real part. The imaginary part of equation (19) can be shown as

$$\begin{bmatrix} I & \omega \end{bmatrix}\begin{bmatrix} D \\ C \end{bmatrix}=\text{imag}\left[H(\omega)^c\right]^{-1} \tag{20}$$

Finally, the damping matrices C and D can be obtained by pseudo-inverse of equation (20)

$$\begin{bmatrix} D \\ C \end{bmatrix}_{2n\times n}=\begin{bmatrix} I & \omega_1 I \\ I & \omega_2 I \\ \vdots & \vdots \\ \vdots & \vdots \\ I & \omega_k I \end{bmatrix}^{+}_{kn\times 2n}\begin{bmatrix} \text{imag}\left[H(\omega_1)^c\right]^{-1} \\ \text{imag}\left[H(\omega_2)^c\right]^{-1} \\ \vdots \\ \text{imag}\left[H(\omega_k)^c\right]^{-1} \end{bmatrix}_{kn\times n} \tag{21}$$

where + means the pseudo-inverse of the matrix.

B. Damping matrices of a single beam model

The complex full FRF matrix was measured with a clamped-clamped beam. The experimental setup is the same with **Figure 3** in section III-C. The 9x9 full FRF matrix was obtained with 9 measurement points. By using the equation (21), the damping matrices of a single beam was calculated such as

Table 6. Viscous damping matrix: C (N s/m)

	1	2	3	4	5	6	7	8	9
1	-0.0018124	0.0011592	0.0003113	-0.00082678	0.00059658	-0.0010402	0.00083864	0.00034757	-0.00083814
2	-6.2658e-05	1.328e-05	-0.00021983	-2.348e-05	0.00011535	0.00023929	-0.0001088	-4.2801e-05	-0.00086291
3	0.00010996	-8.6434e-05	0.0001857	4.7132e-05	-2.9129e-06	-0.00015185	-5.8864e-05	1.7678e-05	0.00056615
4	3.2181e-05	-2.997e-06	-4.1983e-05	7.3048e-05	-3.3086e-05	-5.9301e-05	3.4225e-05	-3.6291e-05	0.00010612
5	-4.7225e-06	1.4639e-05	-0.00019912	7.9781e-05	-0.00013775	0.00020552	7.1104e-05	-0.00014255	2.3086e-05
6	-2.7944e-05	7.5972e-05	1.9912e-05	6.151e-06	5.746e-05	-6.8759e-05	1.696e-05	0.00011011	1.0836e-05
7	-0.00014896	3.177e-05	6.7934e-05	-2.2777e-05	6.8568e-05	-0.00014025	0.00012438	-2.7277e-05	-2.1455e-05
8	-9.923e-05	2.8563e-05	-0.0003389	0.0001473	9.0285e-05	4.5104e-05	-6.0074e-05	-7.8473e-05	-0.00035404
9	-0.0010684	-0.00038676	0.0017091	0.00043266	-0.00070154	-0.0014187	0.00065738	-0.00010954	0.003057

Table 7. Structural damping matrix: D (N/m)

	1	2	3	4	5	6	7	8	9
1	-0.67853	0.45101	0.15552	-0.31214	0.23651	-0.37845	0.30493	0.11844	-0.30007
2	-0.022402	0.0014781	-0.091263	-0.0088955	0.046514	0.089895	-0.040283	-0.011641	-0.32626
3	0.03991	-0.029297	0.063894	0.016647	-0.0061497	-0.049452	-0.020055	0.0056383	0.21323
4	0.011983	0.007416	-0.0072523	0.031087	-0.021549	-0.017871	0.0048495	-0.012307	0.039017
5	-0.0069825	0.024816	-0.073289	0.028265	-0.049014	0.064807	0.021538	-0.049281	0.012523
6	-0.013913	0.036291	0.030548	0.010027	0.016854	-0.032486	0.0063037	0.04495	0.0021203
7	-0.057174	0.027131	0.020737	-0.019201	0.023579	-0.05367	0.040738	-0.013247	-0.0055219
8	-0.038141	0.014045	-0.11908	0.054072	0.034551	0.027519	-0.0076088	-0.018524	-0.13184
9	-0.42273	-0.12425	0.64482	0.16405	-0.28594	-0.51122	0.26492	-0.038956	1.1466

C. Damping matrices of a combined system

A comparison of the obtained damping matrices was conducted with two test specimens to verify the effect of attaching the cable bundle. The specimens are shown in **Figure 11**. In specimen 1, Copper beam (1/8-inch dia.) was treated as a cable bundles. And an electric cable was attached to Aluminum beam in specimen 2. Attached electric cable is shown in **Figure 12**.

Figure 11. Test Specimens: front view(top), specimen 1(middle), and 2(bottom)

Figure 12. Electric cable in specimen 2

By using the equation (21), the damping matrices of the combined systems were calculated. **Table 8**, **9** show the viscous damping matrices of specimen 1, 2. **Table 10Table 11** show the structural damping matrices of specimen 1, 2.

Table 8. Viscous damping matrix of specimen 1: C (N s/m)

	1	2	3	4	5	6	7	8	9
1	0.0002112	0.000465	0.00011749	-0.00029022	-0.00016072	0.00021873	0.00011707	0.00028805	0.00075833
2	-0.00020638	-2.7286e-05	-0.00017578	3.2052e-05	0.00022129	0.00017643	0.00016157	-0.00058665	-0.00011018
3	0.00015628	-5.3529e-05	0.0002842	2.3136e-05	-0.0001998	-8.7489e-05	-0.00011874	0.00036937	3.0244e-05
4	-3.5489e-05	0.0001123	-0.00015932	0.00017199	-3.6639e-06	-5.9577e-06	1.4991e-05	-0.00011206	-9.103e-05
5	9.4382e-05	-5.0421e-05	0.00016689	-0.00011788	1.2861e-05	-0.00010861	-8.9761e-05	0.00028859	7.0342e-05
6	-6.9925e-06	-3.368e-05	4.316e-05	-2.3138e-05	7.2684e-07	-1.3912e-05	6.2963e-05	-6.5373e-06	1.8287e-05
7	-1.4257e-05	8.4066e-05	2.2353e-05	-6.7059e-05	-4.0943e-05	5.8036e-05	-9.217e-05	0.00015638	-3.5083e-05
8	-9.6403e-05	-0.0001417	-0.00032673	0.00030282	0.00025792	8.834e-05	0.0002452	-0.00064797	-2.4724e-05
9	2.7461e-05	-0.00026815	-7.7382e-05	-9.6061e-06	8.8285e-05	2.3088e-05	-4.1612e-05	-1.6101e-05	-0.00079623

Table 9. Viscous damping matrix of specimen 2: C (N s/m)

	1	2	3	4	5	6	7	8	9
1	-0.0068727	0.00050382	0.0029817	-5.0139e-05	0.00010373	-0.0020976	0.00066007	7.8252e-05	0.0059399
2	0.0010792	-3.3739e-05	-0.00049901	2.2046e-05	-5.9744e-05	0.00026122	-0.00010414	1.8882e-05	-0.00058955
3	0.00090496	-4.4023e-05	-0.00017986	-0.00011639	-4.7155e-05	0.0003263	-6.1665e-05	-3.3646e-05	-0.00060403
4	-0.00035206	-2.4831e-05	0.00012846	3.7089e-05	-1.7199e-06	-8.8655e-05	-8.3108e-06	4.2696e-06	0.00023448
5	-0.00065665	6.3473e-07	0.00011994	3.6576e-05	0.0001252	-0.00024264	2.4733e-05	4.1267e-05	0.00038949
6	-0.00012144	1.7689e-05	2.8576e-05	1.4847e-05	-5.3038e-05	-4.36e-05	7.1802e-05	-1.842e-06	-5.3894e-05
7	0.0001941	1.5446e-05	-9.3257e-05	-3.3447e-05	-2.5807e-05	0.00011822	-4.303e-05	2.4419e-06	-0.00012731
8	0.00015933	1.6439e-06	-2.2542e-05	9.1534e-06	-5.4269e-05	3.139e-05	-2.7629e-05	7.8229e-06	-1.0036e-05
9	0.0020779	-0.00016883	-0.00038717	9.6781e-05	0.00029737	-0.00011313	-0.00024543	-2.1636e-05	-0.00024242

Table 10. Structural damping matrix of specimen 1: D (N/m)

	1	2	3	4	5	6	7	8	9
1	0.078787	0.14304	0.015506	-0.10987	-0.042206	0.084764	0.032467	0.13287	0.26095
2	-0.077949	-0.0084654	-0.059285	0.009216	0.079809	0.058877	0.066105	-0.21644	-0.044787
3	0.059358	-0.027804	0.092866	0.0037706	-0.0716	-0.02584	-0.050975	0.13527	0.012787
4	-0.013569	0.039341	-0.060639	0.068321	-0.0050271	-0.0048105	0.013144	-0.039022	-0.037148
5	0.034903	-0.024674	0.06293	-0.042133	0.0053336	-0.042909	-0.035304	0.1092	0.025366
6	-0.0031179	-0.0054326	0.017025	-0.011936	-0.0022765	-0.010294	0.028006	-0.00042103	0.0074266
7	-0.0056185	0.037505	0.0049975	-0.025942	-0.016036	0.02523	-0.040209	0.051497	-0.010357
8	-0.036502	-0.058061	-0.11846	0.11533	0.09899	0.027175	0.097824	-0.24774	-0.0090696
9	0.0044129	-0.065677	-0.058445	-0.00022131	0.028917	0.020886	-0.019149	-0.019009	-0.29835

Table 11. Structural damping matrix of specimen 2: D (N/m)

	1	2	3	4	5	6	7	8	9
1	2.5786	-0.20648	-1.116	0.030149	-0.048319	0.78609	-0.28727	-0.01406	-2.2465
2	-0.40221	0.015279	0.18503	-0.0095088	0.021621	-0.1022	0.041895	-0.0084177	0.22525
3	-0.34054	0.011355	0.078742	0.045408	0.019622	-0.11695	0.0039884	0.016425	0.22611
4	0.1313	0.01326	-0.046907	-0.016118	-0.00092474	0.033508	0.0025948	-0.0051058	-0.088731
5	0.24516	-0.0073319	-0.046298	-0.015005	-0.046305	0.088978	-0.019661	-0.013667	-0.14567
6	0.044257	-0.0092782	-0.017398	-0.0056502	0.016574	0.011596	-0.03423	0.0028583	0.020936
7	-0.072958	-0.00047667	0.033278	0.013796	0.0069839	-0.047196	0.019561	-0.0020507	0.050059
8	-0.059798	-0.0037793	0.0073318	-0.0029246	0.021138	-0.015099	0.0054632	0.0019825	0.004477
9	-0.80011	0.074302	0.14423	-0.044887	-0.11469	0.051796	0.10699	0.0081979	0.083651

D. Comparison of the damping matrices

Figure 13 shows the viscous damping matrices C. After connection occurs, the viscous damping coefficients were decreased in specimen 1. The viscous damping matrix increases in specimen 2. The same phenomenon was found in the structural damping matrices D as shown in **Figure 14**. The norms of matrices are summarized in **Table 12**. From these results, it can be concluded that the type of cables can affect the damping. Because the real cable bundle, that applied in the satellite structures, are twisted and wrapped together. The damping effect due to adding a cable bundle will be closer with specimen 2. This means that the real structure will experience the increase of damping.

Table 12. Norms of damping matrices

Norm	Single Al beam (Base structure)	Al beam + Copper beam (Specimen 1)	Al beam + Electric cable (Specimen 2)
Viscous damping (N s/m)	0.0051867	0.0019407	**0.010269**
Structural damping (N/m)	1.9507	0.71062	**3.871**

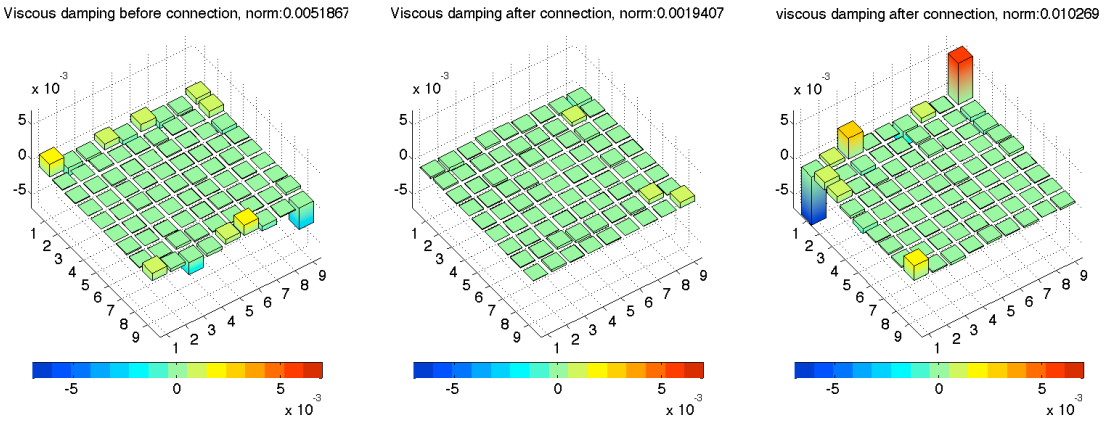

Figure 13. Viscous damping matrix: single beam (left), specimen 1 (center), and specimen 2(right)

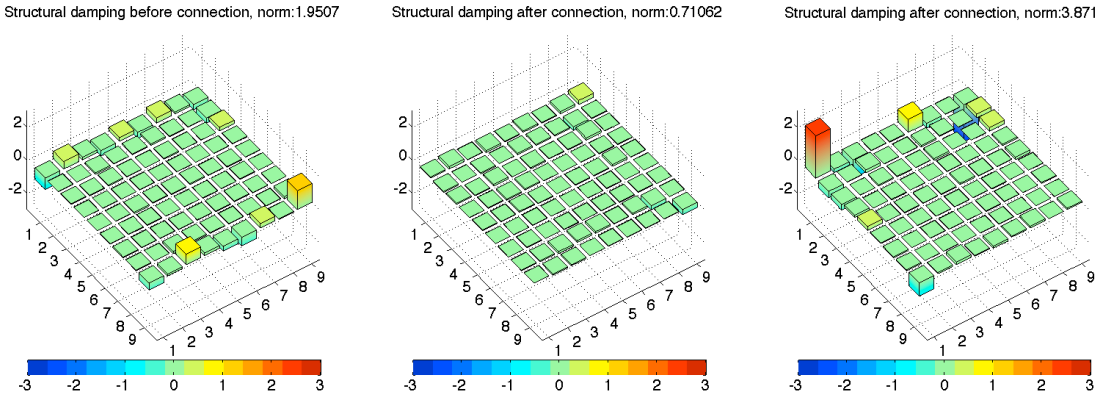

Figure 14. Structural damping matrix: single beam (left), specimen 1 (center), and specimen 2(right)

VI. Conclusion

In this paper, the Spectral Element Method (SEM) approach is proposed to model the dynamics of a cable harnessed structure. From numerical analysis and experiments, SEM was validated providing an accurate model for a dynamics of a combined system. In addition the damping effect due to attaching a cable bundle was investigated by calculating the damping matrices from the measured complex FRF matrix. Two types of cable attachments are considered. We can conclude that the type of cables can affect the damping differently. The damping in real structures will increase by adding a cable bundle.

Acknowledgments

Authors gratefully acknowledge the support from the (US) Air Force Office of Scientific Research grant number FA9550-10-1-0427 titled “Structural Dynamics of Cable-Harnessed Spacecraft Structures” monitored by Dr. David Stargel.

References

[1]Inman, D. J. *Engineering vibration*: 4th Edition, Pearson Prentice Hall, 2013.

[2]Hoppmann, J. M. S. W. H., and Ii. "Normal Mode Vibrations of Systems of Elastically Connected Parallel Bars," *The Journal of the Acoustical Society of America* Vol. 36, No. 1, 1964, pp. 93-99.

[3]Gürgöze, M. "On the Eigenfrequencies of A Cantilver Beam with Attached Tip Mass and A Spring-mass System," *Journal of Sound and Vibration* Vol. 190, No. 2, 1996, pp. 149-162.

[4]Gürgöze, M. "On the Alternative Formulations of the Frequency Equation of A Bernoulli–Euler Beam to which Several Spring-mass Systems Are Attached In-span," *Journal of Sound and Vibration* Vol. 217, No. 3, 1998, pp. 585-595.

[5]Vu, H. V., OrdÓÑEz, A. M., and Karnopp, B. H. "Vibration of A Double-beam System," *Journal of Sound and Vibration* Vol. 229, No. 4, 2000, pp. 807-822.

[6]Wu, J. S., and Chou, H. M. "Free Vibration Analysis of A Cantilever Beam Carrying Any Number of Elastically Mounted Point Masses with the Analytical-and-numerical-combined Method," *Journal of Sound and Vibration* Vol. 213, No. 2, 1998, pp. 317-332.

[7]Coombs, D. M. G., J.C. ; Babuska, V.; Ardelean, E.V.; Robertson, L.M.;Lane, S.A. "Dynamic Modeling and Experimental Validation of a Cable-Loaded Panel," *Journal of Spacecraft and Rockets* Vol. 48, 2011, pp. 958-973.

[8]Rao, S. S. "Natural vibrations of systems of elastically connected Timoshenko beams," *The Journal of the Acoustical Society of America* Vol. 55, No. 6, 1974, pp. 1232-1237.

[9]Doyle, J. F. *Wave propagation in structures: spectral analysis using fast discrete Fourier transforms*. New York: Springer, 1997.

[10]Lee, U. *Spectral element method in structural dynamics*. Singapore ; Hoboken, NJ: J. Wiley & Sons Asia, 2009.

[11]Banerjee, J. R. "Dynamic stiffness formulation and its application for a combined beam and a two degree-of-freedom system," *Journal of vibration and acoustics* Vol. 125, No. 3, 2003, pp. 351-358.

[12]Chen, D.-W. "The exact solution for free vibration of uniform beams carrying multiple two-degree-of-freedom spring–mass systems," *Journal of Sound and Vibration* Vol. 295, No. 1–2, 2006, pp. 342-361.

[13]Li, J., and Hua, H. "Spectral finite element analysis of elastically connected double-beam systems," *Finite Elements in Analysis and Design* Vol. 43, No. 15, 2007, pp. 1155-1168.

[14]Jiao, S., Li, J., Hua, H., and Shen, R. "A spectral finite element model for vibration analysis of a beam based on general higher-order theory," *Shock and Vibration* Vol. 15, No. 2, 2008, pp. 179-192.

[15]Li, J., and Hua, H. "Dynamic stiffness vibration analysis of an elastically connected three-beam system," *Applied Acoustics* Vol. 69, No. 7, 2008, pp. 591-600.

[16]Lee, J. H. "Development of New Technique for Damping Identification and Sound Transmission Analysis of Various Structures." University of Cincinnati, 2001.

[17]Lee, J. H., and Kim, J. "Identification of Damping Matrices from Measured Frequency Response Functions," *Journal of Sound and Vibration* Vol. 240, No. 3, 2001, pp. 545-565.

[18]Burden, R. L., and Faires, J. D. *Numerical analysis*. Belmont, CA: Thomson Brooks/Cole, 2005.

[19]Choi, J. D., and Inman, D. J. "Spectral Element Method for Cable Harnessed Structure," *Proceedings of International Modal Analysis Conference XXXI*, Orange County, CA, 2013.